Conference Paper

Wind-Tunnel Tests of Two Airfoils for Wind Turbines Operating at High Reynolds Numbers

Dan M. Sommers
Airfoils Incorporated

James L. Tangler
National Renewable Energy Laboratory

NREL

National Renewable Energy Laboratory

1617 Cole Boulevard
Golden, Colorado 80401-3393

Wind-Tunnel Tests of Two Airfoils for Wind Turbines
Operating at High Reynolds Numbers

Dan M. Somers
Airfoils Incorporated
122 Rose Drive
Port Matilda, Pennsylvania 16870-9483

James L. Tangler
National Renewable Energy Laboratory
1617 Cole Boulevard
Golden, Colorado, 80401-3393

Abstract

The objectives of this study were to verify the predictions of the Eppler Airfoil Design and Analysis Code for Reynolds numbers up to 6×10^6 and to acquire the section characteristics of two airfoils being considered for large, megawatt-size wind turbines. One airfoil, the S825, was designed to achieve a high maximum lift coefficient suitable for variable-speed machines. The other airfoil, the S827, was designed to achieve a low maximum lift coefficient suitable for stall-regulated machines. Both airfoils were tested in the NASA Langley Low-Turbulence Pressure Tunnel (LTPT) for smooth, fixed-transition, and rough surface conditions at Reynolds numbers of 1, 2, 3, 4, and 6×10^6. The results show the maximum lift coefficient of both airfoils is substantially underpredicted for Reynolds numbers over 3×10^6 and emphasized the difficulty of designing low-lift airfoils for high Reynolds numbers.

Symbols

C_p pressure coefficient
c airfoil chord
c_d section profile drag
c_l section lift coefficient
c_m section moment coefficient
L.   lower surface
R   Reynolds number
S.   boundary-layer separation point
T.   boundary-layer transition location
U.   upper surface
x   airfoil abscissa
α angle of attack relative to airfoil chord

Subscripts

ll   lower limit of low-drag range
max   maximum
min   minimum
ul   upper limit of low-drag range

Introduction

Verification of codes used for the design of wind-turbine airfoils, such as the Eppler Airfoil Design and Analysis Code[1], has been limited to Reynolds numbers below 3×10^6 by the unavailability of high-Reynolds-number, wind-tunnel facilities. With the recent trend toward larger turbines, rated at over one megawatt, the currently available airfoil data are inadequate for the purpose of designing or predicting rotor performance. In addition, high-Reynolds-number, airfoil-code verification is needed for the prediction of both the maximum lift coefficient ($c_{l,\max}$) and the width and depth of the low-drag range.

The NASA Langley Low-Turbulence Pressure Tunnel (LTPT)[2,3] was used for this study because it is the only two-dimensional wind tunnel capable of chord Reynolds numbers greater than 4×10^6 with low turbulence ($\leq 0.05\%$). Two airfoils, the S825 and S827, from the National Renewable Energy Laboratory (NREL) airfoil families[4] were tested. Each airfoil was tested for smooth, fixed transition, and rough surface conditions at Reynolds number of 1, 2, 3, 4, and 6×10^6.

This paper is condensed from the two reports, which includes the airfoil coordinates, covering this study.[5,6]

Airfoils

The 17-percent thick S825 airfoil was designed to achieve a high maximum lift coefficient (≥ 1.40) suitable for variable-speed wind turbines. The 21-percent thick S827 airfoil was designed to achieve a low (restrained) maximum lift coefficient ($\cong 1.00$) suitable for large, stall-regulated machines. Both airfoils were designed to achieve extensive laminar flow (≥ 30-percent chord) on both the upper and lower surfaces for low drag. Transition to turbulent flow moves to the leading edge just prior to reaching maximum lift, which minimizes the effect of roughness on the maximum lift coefficient. Both airfoils were designed to exhibit benign laminar separation bubbles near the leading edge at maximum lift coefficient. More severe bubbles can lead to unpredictable and erratic

maximum-lift-coefficient behavior. The design specifications for the two airfoils are shown in Table 1 and the airfoil shapes are shown in Fig. 1.

Experimental Procedure

Wind Tunnel
The NASA Langley Low-Turbulence Pressure Tunnel (LTPT) is a closed-throat, single-return tunnel (Fig. 2) that can be operated at stagnation pressures from 100 to 1000 kPa (1 to 10 atm). The unit Reynolds number can be varied from 1×10^6 to 49×10^6 per meter (0.3×10^6 to 15×10^6 per foot); the Mach number can be varied from 0.05 to 0.47. The turbulence level in the test section[7] is generally below 0.05 percent for unit Reynolds number up to 13×10^6 per meter (4×10^6 per foot) at Mach numbers up to 0.15.

The wind tunnel test section is 91 cm (36 in.) wide by 229 cm (90 in.) high. Hydraulically actuated circular plates provide positioning and attachment for the two-dimensional model (Fig. 3). The plates are flush with the tunnel sidewalls and rotate with the model. The axis of rotation coincided approximately with the midchord of the model, which was mounted horizontally between the plates. The gaps between the model and the plates were sealed.

Models
Advanced Technologies, Incorporated, Newport News, Virginia fabricated the two wind-tunnel models from solid aluminum using a numerically controlled milling machine. The models had a chord of 457 mm (18.0 in.) and a span of 91 cm (36.0 in.). The measured model contours were within 0.1 mm (0.005 in.) of the prescribed shapes.

Each model included a total of 120 chordwise pressure ports over the upper and lower surface. Upper- and lower-surface orifices were located to one side of midspan, staggered along a line approximately 10 degrees from the free steam flow direction. All the orifices were 0.51 mm (0.020 in.) in diameter with their axes perpendicular to the airfoil surface.

Instrumentation
Measurements of the pressures on the model and in the wake were made by an electronically scanned, pressure-transducer system. Basic tunnel pressures were measured with precision quartz manometers. Data were recorded by an electronic data-acquisition system.

Methods
The measured pressure distributions were integrated to determine the lift coefficients. Profile drag was measured using a total- and static-pressure, wake-survey probe. The probe was positioned spanwise at the tunnel centerline. The tip of the probe was located 1.84 chord downstream of the trailing-edge of the model and could traverse the entire wake profile.

Standard, low-speed, wind-tunnel boundary corrections[8] have been applied to the data, along with the wake-survey-probe total-pressure-tube displacement correction[9].

Tests
The models were tested at Reynolds numbers, based on airfoil chord, of 1, 2, 3, 4, and 6×10^6 and a Mach number of 0.1 with transition free (smooth), with transition fixed, and with a grit roughness scaled from NACA standard roughness[10]. Transition was fixed using grit roughness that decreased in size with increasing Reynolds number.[11] as seen in Table 2. The grit was located at 2-percent chord on the upper surface and 5-percent chord on the lower surface. It was sparsely distributed along 3-mm (0.1-in.) wide strips applied to the model with lacquer. The scaled, NACA standard roughness consisted of 0.211-mm (0.0083-in.) grit applied from 8-percent-chord arc length on the upper surface to 8-percent-chord arc length on the lower surface for all Reynolds numbers. The grit size was scaled from the NACA standard-roughness grit size by the ratio of the model chord used in the present investigation to the model chord used in the NACA tests.

Results

Pressure Distributions
Typical measured pressure distributions for the S825 and S827 airfoils are shown in Fig. 4 for an angle of attack of 3.0 degrees. The integrated pressure distributions then yielded c_l versus angle of attack plots, which were documented for the complete test matrix.

Section Characteristics of S825 Airfoil
The theoretical and experimental section characteristics of the S825 airfoil for the design Reynolds number of 2×10^6 are shown in Fig. 5. The measured maximum lift coefficient is 1.56, which satisfies the design objective of $c_{l,max} \geq 1.40$. The airfoil exhibits a rapid, trailing-edge

stall, which does not meet the design goal of docile stall characteristics. Low profile-drag coefficients are exhibited over the range of lift coefficients from 0.05 to 1.10. The lower limit of the low-drag range is below the design objective of $c_{l,ll} = 0.40$ although the upper limit is also below the design objective of $c_{l,ul} = 1.20$, primarily to meet other, more important goals. The drag coefficient at $c_l = 0.40$ is 0.0068, which satisfies the design objective of $c_{d,min} \leq 0.0080$. The zero-lift pitching-moment coefficient is -0.15, which satisfies the design constraint of $c_{m,0} \geq$ -0.15.

Comparisons of the predicted and measured section characteristics generally show the magnitudes of the zero-lift angle, the pitching moment coefficient, and the width of the low-drag range are overpredicted. The maximum lift coefficient is underpredicted.

Section Characteristics of S827 Airfoil
The theoretical and experimental section characteristics of the S827 airfoil for the design Reynolds number of 4×10^6 are shown in Fig. 6. The measured maximum lift coefficient is 1.28, which substantially exceeds the design objective of $c_{l,max} \cong 1.00$. Low profile-drag coefficients are exhibited over the range of lift coefficients from 0.04 to 0.75. The lower limit of the low-drag range is below the design objective of $c_{l,ll} = 0.20$ although the upper limit is also below the design objective of $c_{l,ul} = 0.80$, primarily to meet other, more important goals. The drag coefficient at $c_l = 0.20$ is 0.0049, which satisfies the design objective of $c_{d,min} \leq 0.008$. The zero-lift pitching-moment coefficient is -0.07, which satisfies the design constraint of $c_{m,0} \geq$ -0.07.

Comparison of predicted and measured section characteristics generally shows the magnitudes of the zero-lift angle and the pitching moment coefficient are overpredicted. The width of the low-drag range is also overpredicted. The maximum lift coefficient is significantly underpredicted with increasing Reynolds number.

Effect of Roughness
The effect of fixing transition on the section characteristics is shown in Figs. 7 and 8 for the S825 and S827 airfoils, respectively. In general, the lift-curve slope, the maximum lift coefficient, and the magnitudes of the zero-lift angle of attack and the pitching-moment coefficients decrease with transition fixed. These results are primarily a consequence of the boundary-layer displacement effect, which decambers the airfoil, the displacement thickness being greater with transition fixed than with transition free. In addition, the lift-curve slope and the maximum lift coefficient decrease with transition fixed because the roughness induces early trailing-edge separation, particularly at high angles of attack. Both airfoils exhibit no hysteresis for angles of attack beyond stall. The maximum lift coefficient of the S825 airfoil for the design Reynolds number of 2×10^6 is 1.52, a reduction of less than 3 percent from that with transition free. The maximum lift coefficient of the S827 airfoil for the design Reynolds number of 4×10^6 is 1.26, a reduction of less than 2 percent from that with transition free. The drag coefficients are, of course, adversely affected by the roughness.

The effect of the scaled, NACA standard roughness on the section characteristics is more severe than that of fixing transition. The maximum lift coefficient of the S825 airfoil for the design Reynolds number of 2.0×10^6 is 1.34, a reduction of 14 percent from that with transition free. The maximum lift coefficient of the S827 airfoil for the design Reynolds number of 4×10^6 is 1.06, a reduction of 17 percent from that with transition free. The greater reduction of 17 percent for the S827 airfoil versus 14 percent for the S825 may be attributed to two effects. First, roughness losses have been found to be proportional to airfoil thickness[12]. Second, the effect of roughness is proportional to the ratio of the roughness height to the boundary-layer thickness. Because the roughness height of the scaled, NACA standard roughness and the airfoil chord are constant, the effect of this roughness generally increases with increasing Reynolds number (because the boundary-layer thickness decreases with increasing Reynolds number).

Reynolds Number Effects
The variation of maximum lift coefficient with Reynolds number for the S825 and S827 airfoils is shown in Figs. 9 and 10, respectively. The maximum lift coefficient increases with increasing Reynolds number. The rate of increase is similar with transition free and transition fixed but lower with the scaled, NACA standard roughness.

The variation of profile-drag coefficient with Reynolds number is shown in Fig. 11 and Fig. 12 for the S825 and S827, respectively. For both airfoils the drag coefficient generally decreases with increasing Reynolds number, except at a Reynolds number of 1×10^6, when bubble drag is decreased from early boundary layer transition.

Conclusions

Comparisons of the theoretical and experimental airfoil section characteristics illustrate weaknesses in the theoretical methodology. The most significant discrepancy is in the prediction of the maximum lift coefficient, which is substantially underpredicted by the Eppler code for both the low and high lift airfoils. This discrepancy becomes larger with increasing Reynolds number. Another discrepancy was the prediction of a wider drag bucket relative to measurements.

For the high-lift S825 airfoil, the measured maximum lift coefficient is somewhat higher than the predicted value. The airfoil exhibits a rapid, trailing-edge stall, rather than the goal of docile stall characteristics. The measured minimum drag and pitching moment coefficient agreed favorably with predictions.

For the low-lift S827 airfoil, the measured maximum lift coefficient is substantially higher than the predicted value. This comparison emphasizes the difficulty of designing a low-lift airfoil for high Reynolds numbers. The measured minimum drag and pitching moment coefficient agreed favorably with predictions.

References

[1]Eppler, R., 1998, "Airfoil Program System "PROFIL98." User's Guide," c. 1998.

[2]Von Doenhoff, A. E., and Abbott, F. T., Jr., "The Langley Two-Dimensional Low-Turbulence Pressure Tunnel," NACA TN 1283, 1947.

[3]McGhee, R. J., et al., "Recent Modifications and Calibration of the Langley Low-Turbulence Pressure Tunnel," NASA TP-2328, 1984.

[4]Tangler, J. L., and Somers, D. M., "NREL Airfoil Families for HAWTs," American Wind Energy Association WindPower '95, Washington, DC, 1995.

[5]Somers, D. M., "Design and Experimental Results for the S825 Airfoil," NREL Report to be published 1999.

[6]Somers, D. M., "Design and Experimental Results for the S827 Airfoil," NREL Report to be published 1999.

[7]Wlezien, R. W., et al., "Comparison of Flow Quality in Subsonic Pressure Tunnels," AIAA Paper 94-2503, 1994.

[8]Allen, H. J., and Vincenti, W. G., "Wall Interference in a Two-Dimensional-Flow Wind Tunnel, With Consideration of the Effect of Compressibility," NACA Rep. 782, 1944.

[9]Pankhurst, R. C., and Holder, D. W., "Wind-Tunnel Technique," Sir Isaac Pitman & Sons, Ltd. (London), 1965.

[10]Abbott, I. H., Von Doenhoff, A. E., and Stivers, L. S., Jr., "Summary of Airfoil Data," NACA Rep. 824, 1945.

[11]Braslow, A. L. and Knox, E. C., "Simplified Method for Determination of Critical Height of Distributed Roughness Particles for Boundary-Layer Transition at Mach Numbers From 0 to 5," NACA TN 4363, 1958.

[12]Tangler, J. L., and Somers, D. M., "Effect of Airfoil Thickness and Maximum Lift on Roughness Sensitivity," 3rd ASME JSME Joint Fluids Engineering Conference, San Francisco, CA, 1999.

Table 1. Airfoil Design Specifications.

Airfoil	S825	S827
Parameter	Objective/Constraint	
Reynolds number R	2×10^6	4×10^6
Maximum lift coefficient $c_{l,max}$	≥ 1.40	$\cong 1.00$
Lower limit of low drag, lift coefficient range $c_{l,ll}$	0.40	0.20
Upper limit of low-drag, lift coefficient range $c_{l,ul}$	1.20	0.80
Minimum profile-drag coefficient $c_{d,min}$	≤ 0.0080	≤ 0.0080
Zero-lift pitching-moment coefficient $c_{m,0}$	$\geq$ -0.15	$\geq$ -0.07
Airfoil thickness t/c	17%	21%
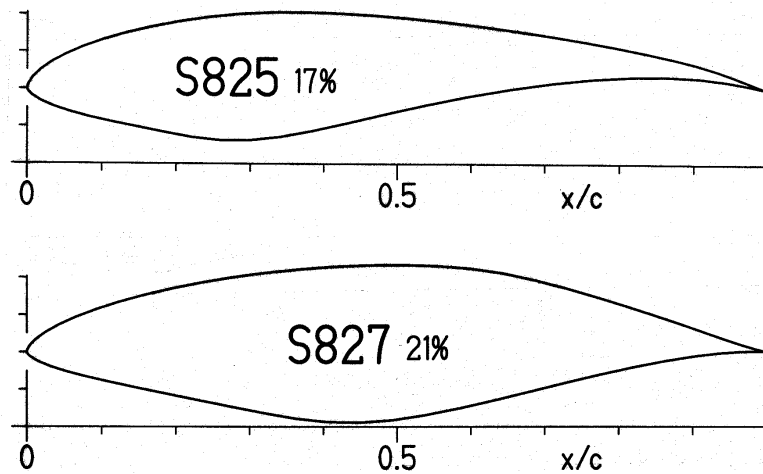
Fig. 1. S825 and S827 airfoil shapes.
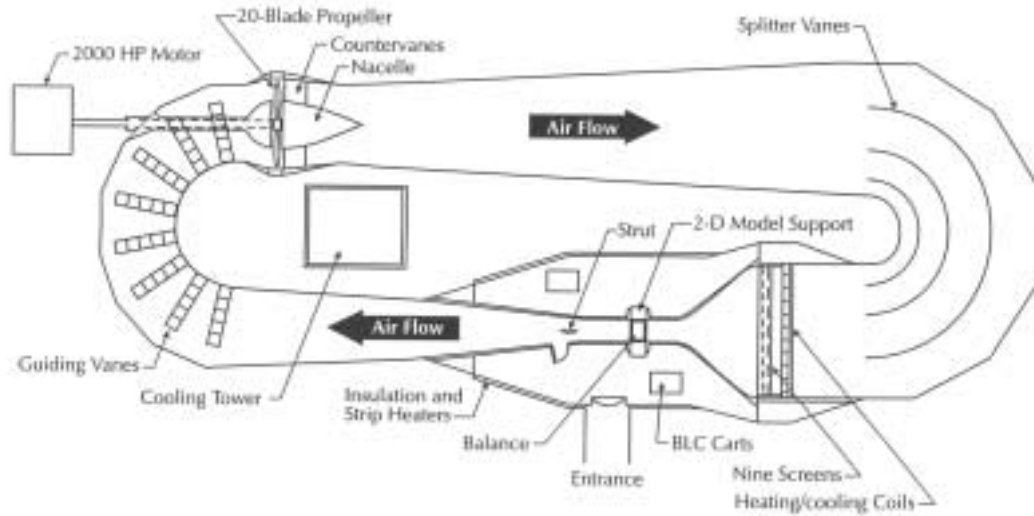
Fig 2. The NASA Langley Low Turbulence Pressure Tunnel.

Table 2. Roughness Location and Size.

Reynolds Number	Upper Surface		Lower Surface	
	x/c	Grit Number/Size	x/c	Grit Number/Size
1.0×10^6	0.02	90/0.178mm (0.0070in.)	0.05	54/0.351mm (0.0138in.)
2.0×10^6		180/0.089mm (0.0035in.)		80/0.211mm (0.0083in.)
3.0×10^6				100/0.150mm (0.0059in.)
4.0×10^6		220/0.074mm (0.0029in.)		
6.0×10^6				180/0.089mm (0.0035in.)

Fig. 3. LTPT test section.
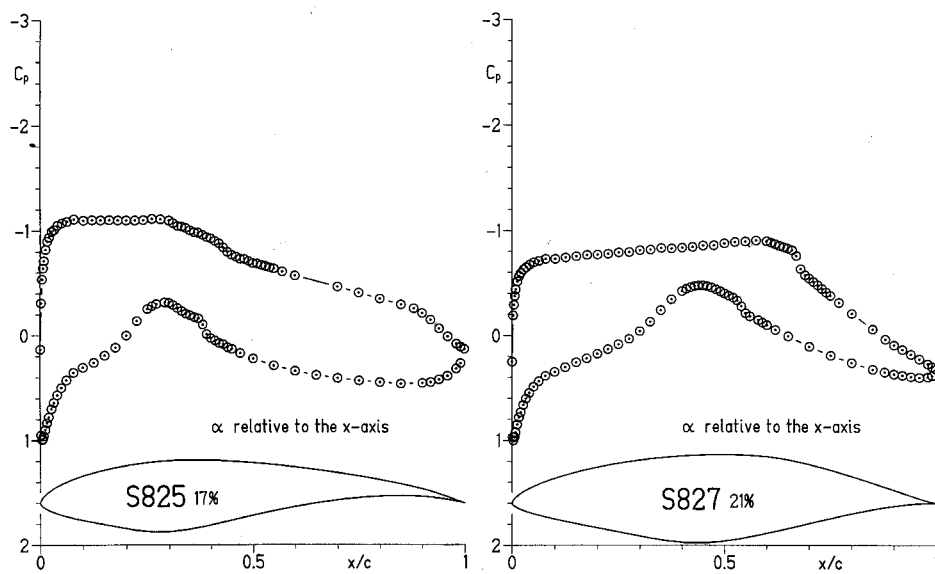
Fig. 4. Typical pressure distributions ($\alpha = 3.0°$).

8
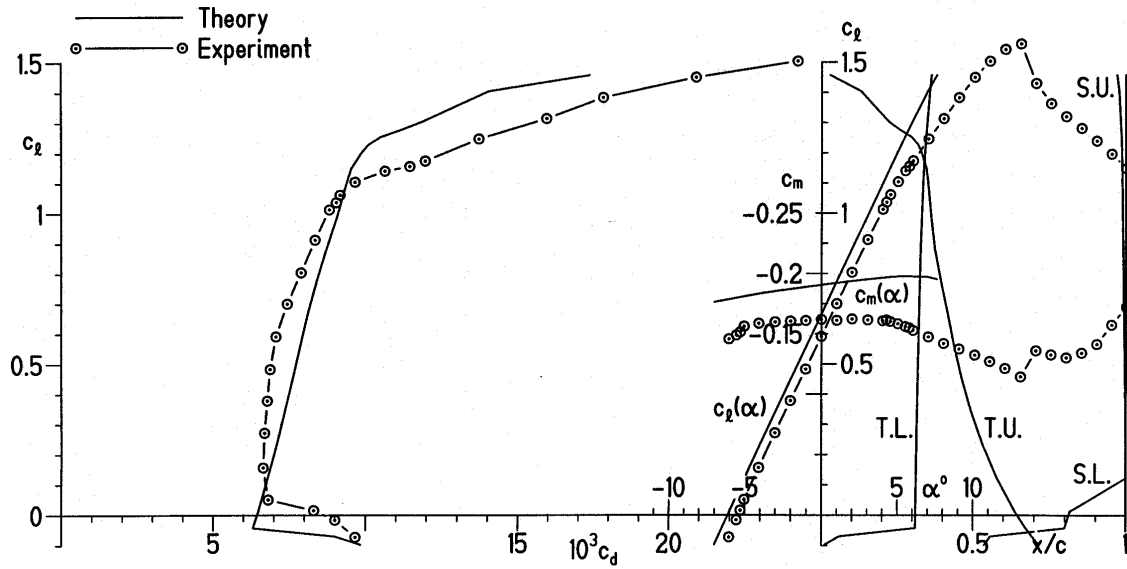
Fig. 5. Comparison of theoretical and experimental section characteristics of S825 airfoil with transition free for design Reynolds number of 2×10^6.
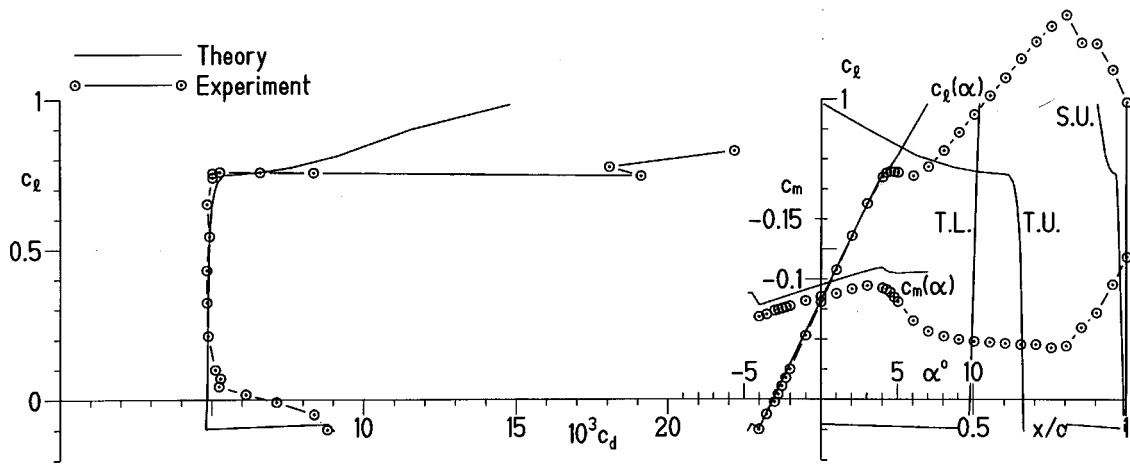
Fig. 6. Comparison of theoretical and experimental section characteristics of S827 airfoil with transition free for design Reynolds number of 4×10^6.
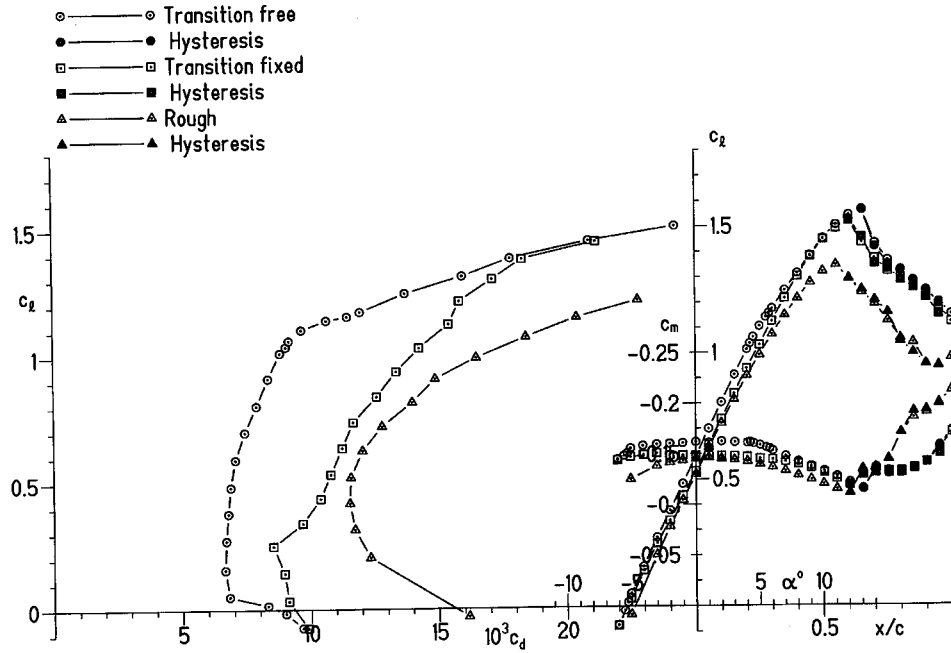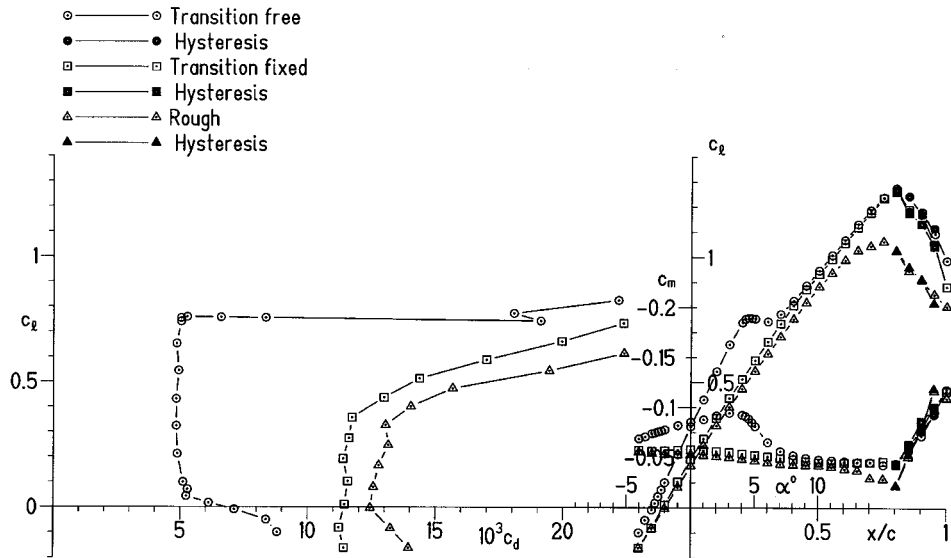
Fig. 7. Section characteristics of S825 airfoil with transition free, transition fixed, and scaled, NACA standard roughness for design Reynolds number of 2×10^6.

Fig. 8. Section characteristics of S827 airfoil with transition free, transition fixed, and scaled, NACA standard roughness for design Reynolds number of 4×10^6.
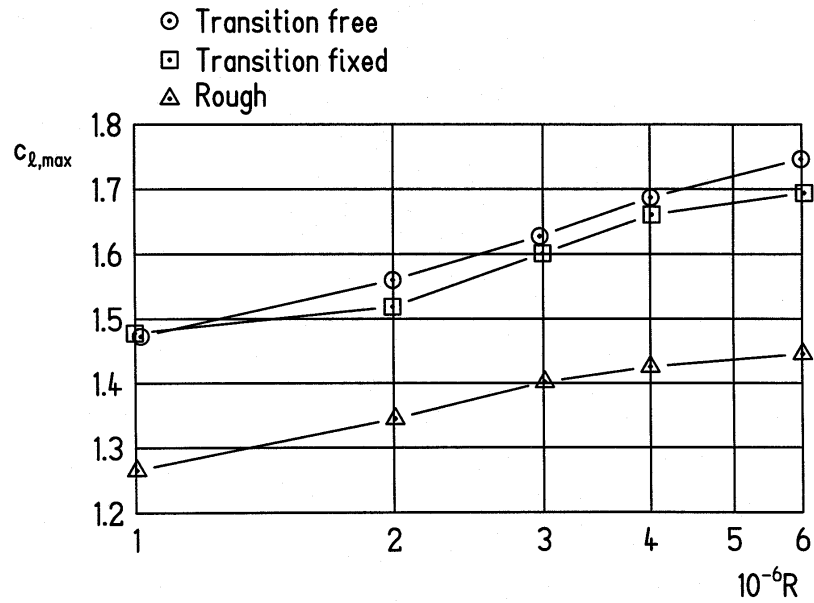
10

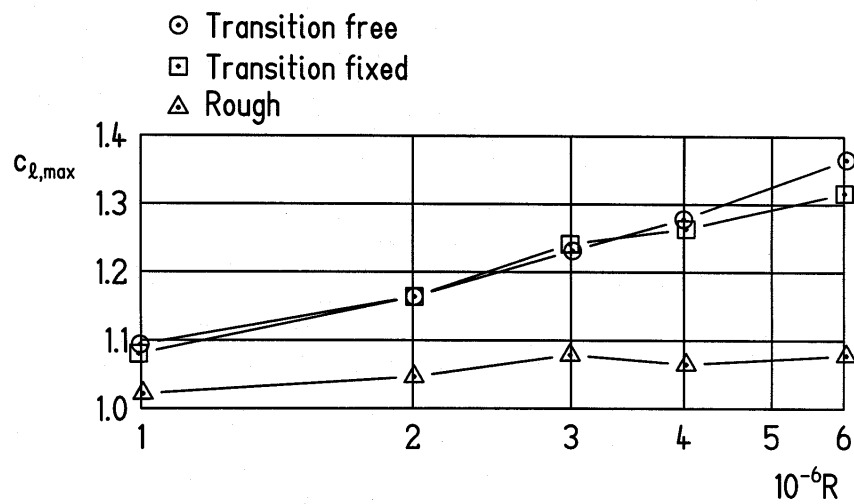Fig. 9. Variation of maximum lift coefficient with Reynolds number for S825 airfoil.

Fig. 10. Variation of maximum lift coefficient with Reynolds number for S827 airfoil.
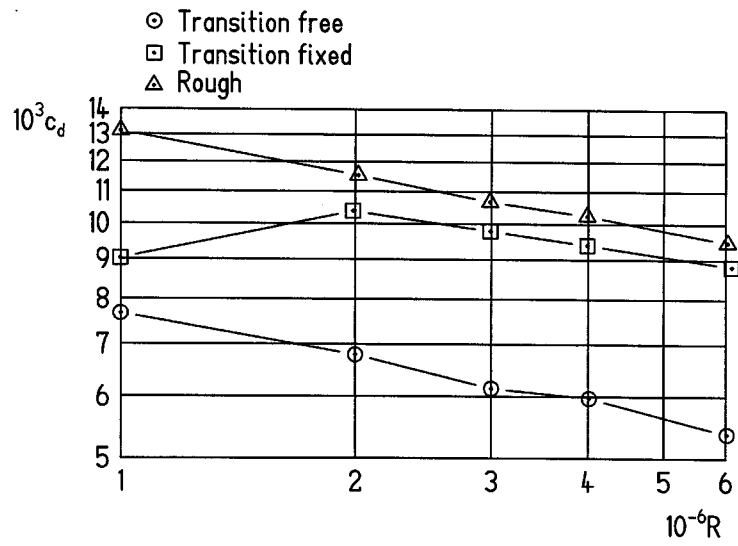
11

Fig. 11. Variation of profile-drag coefficient at $c_l = 0.4$ with Reynolds number for S825 airfoil.
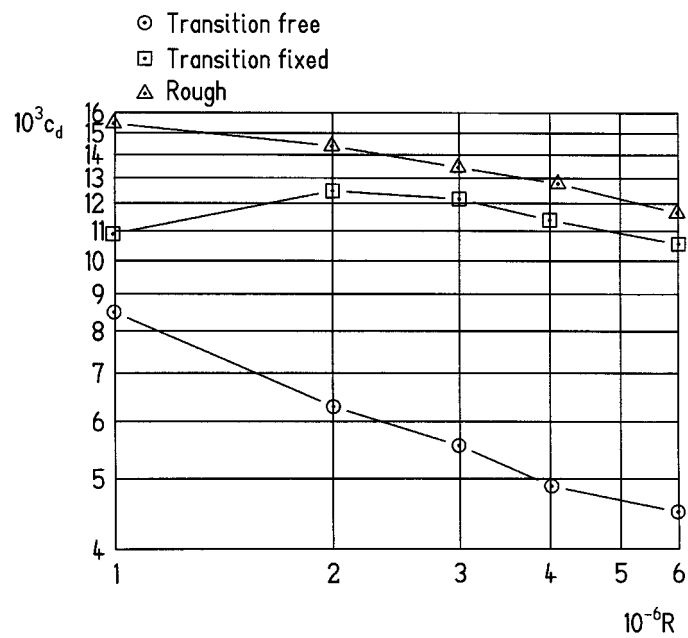

Fig. 12. Variation of profile-drag coefficient at $c_l = 0.2$ with Reynolds number for S827 airfoil.